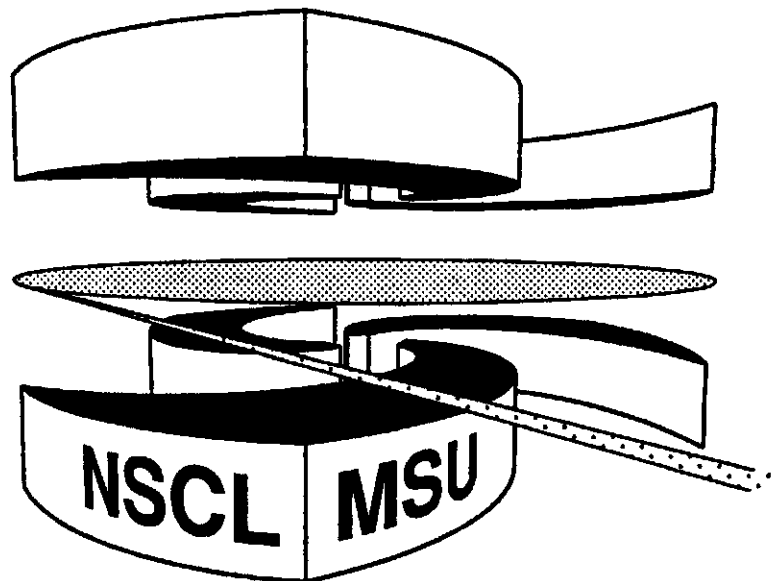


**MICHIGAN STATE**  
**UNIVERSITY**

**National Superconducting Cyclotron Laboratory**

**NUMERICAL STUDY OF THE INJECTION LINE FOR THE  
UNIVERSITY OF MARYLAND ELECTRON RING**

**L.G. VOROBIEV and R.C. YORK**



**MSUCL-1136**

**OCTOBER 1999**

# NUMERICAL STUDY OF THE INJECTION LINE FOR THE UNIVERSITY OF MARYLAND ELECTRON RING \*

L.G.Vorobiev and R.C.York

National Superconducting Cyclotron Laboratory  
Michigan State University  
East Lansing, MI 48824

## *Abstract*

The dynamics of beam injection into the University of Maryland electron ring (UMd E-Ring) have been evaluated. Two recently developed computational tools were employed: a fitting algorithm, based on a generalized set of rms-envelope equations and a Particle-in-Cell (PIC) code. Both models include the effects of momentum dispersion and space charge. The envelope-based fitting algorithm was used to provide the matched beam conditions for the periodical E-Ring structure. These optical conditions were then compared to those obtained from the PIC code tracking both in free space and in the presence of a conducting boundary.

## 1. Introduction

The University of Maryland Electron Ring (E-Ring)\* will operate in the space charge dominated regime. With electron energies of 10 KeV and beam currents of 100 mA, the dimensionless perveance (Q) will be  $1.5 \times 10^{-3}$ . Since the research goal is to determine the physics of space charge dominated beams, the avoidance of effects due to mismatched injection will simplify the experimental determination of the parameter relationships. Our previous studies of the injection line design<sup>2</sup> were based on a generalized set of rms envelope equations that evolved the six parameters  $\sigma_{x,y}$ ,  $\sigma'_{x,y}$  (envelopes and slopes) and  $D_x$ ,  $D'_x$  (horizontal dispersion and its slope) using a coupled set of six differential equations. These analyses showed significant effects arising from incomplete beam matching at injection.

## 2. Conditions Evaluated

Three different beam conditions were considered.

1.  $Q=5 \times 10^{-4}$ ,  $\sigma_\delta=5 \times 10^{-3}$
2.  $Q=10^{-3}$ ,  $\sigma_\delta=10^{-2}$
3.  $Q=1.5 \times 10^{-3}$ ,  $\sigma_\delta=1.5 \times 10^{-2}$

Where  $\sigma_\delta = \sqrt{\langle \delta^2 \rangle}$  denotes the averaged momentum spread (See reference 3.)

---

\* Work supported by the U.S. Department of Energy Contract # DE-FG02-99ER41118

An injection system layout consisting of two dipoles and 8 quadrupoles is shown in Figure 1 where the quadrupoles were assumed to be of the same type as those for the E-Ring. The first dipole deflects the beam by  $20^\circ$  with a second dipole providing a  $-10^\circ$ . The ring injection is at the dipole magnet labeled D1. The initial transverse rms envelopes  $\sigma_{x,y}$  were assumed to be 2 mm. For the third case, the initial transverse rms envelopes  $\sigma_{x,y}$  of 1 mm were also evaluated and found to give similar results. Other beam parameters were as in reference 2.

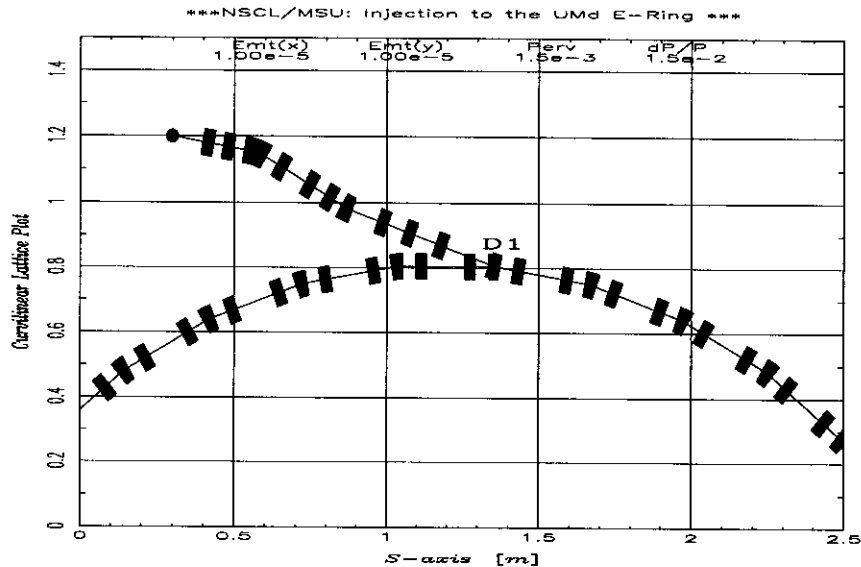


**Figure 1.** Injection lattice and several sectors of the E-ring lattice. Both scales are in meters. The blackened circle denotes the input point into the injection system.

### 3. Envelope-based Analysis

A fitting procedure with the envelope-based code was used for each of the three beam conditions to adjust the initial beam parameters to those corresponding to periodical solutions in the E-ring. Shown in Figure 2 are the rms beam envelopes and horizontal dispersion function through the injection system and the first ten periods of the E-ring for the first case. Similar results were obtained for the other two cases.

For the three cases evaluated, the ratio of  $Q/\sigma_\delta$  is 0.1. Under these conditions, the required injection lattice parameters were similar. Additional cases where  $Q/\sigma_\delta$  was  $>0.1$  were evaluated, and it was found that a longer injection lattice was required to easily achieve the required matched conditions. This suggests that consideration should be given to the operational regime to ensure that the injection system may achieve matched injection for the likely range of beam parameters.

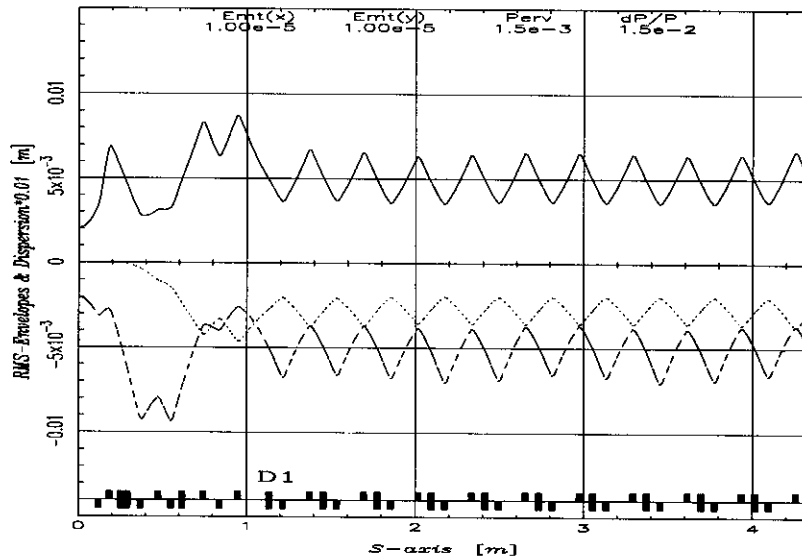


**Figure 2.** RMS beam envelopes  $\sigma_x$  (solid line - horizontal) and  $\sigma_y$  (dashed line - vertical) and dispersion function  $D_x$  (dotted line) for  $Q = 1.5 \times 10^{-3}$  and  $\sigma_\delta = 1.5 \times 10^{-2}$ . The rms emittances are:  $\epsilon_{x,y} = 10^{-5} \pi$  m-rad.

#### 4. Particle-in-Cell Simulations

The 2-D PIC code was recently upgraded to include:

- Arbitrary conducting boundary, e.g. free space, rectangular, circular (see Figure 3), or elliptical.
- Sector dipole, quadrupole, sextupole, and octupole magnets (hard-edge model).
- Initial phase space  $(x, x')$  distributions such as KV, water bag, or parabolic.
- Appropriately addressed momenta dispersion.
- A 4-th order motion equations integrator.

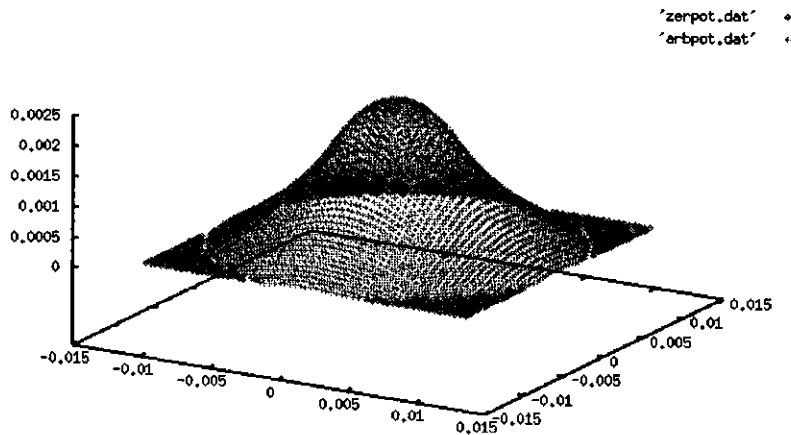


**Figure 3.** The space charge potential of the beam in a round metal pipe (elliptical and rectangular boundaries are also available in the PIC code).

The upgraded PIC code was used to further evaluate the injection systems designed using the envelope-based analysis. Particles with an initial KV distribution in the phase space  $(x, p_x, y, p_y)$  were tracked through the injection system and through 10 periods of the 36 period E-Ring using both free space and a conducting boundary. Figure 4 shows the results of particle simulation for the 3<sup>rd</sup> case for free space. Similar results were obtained for the case of a conducting boundary of 4.9 cm inner diameter. Note, that since the rms envelopes are the 2<sup>nd</sup> moment of the distribution function that depend primarily on the linear part of the external and space charge forces, this agreement might have been anticipated given the relatively short injection system and the inclusion of only 10 ring cells.

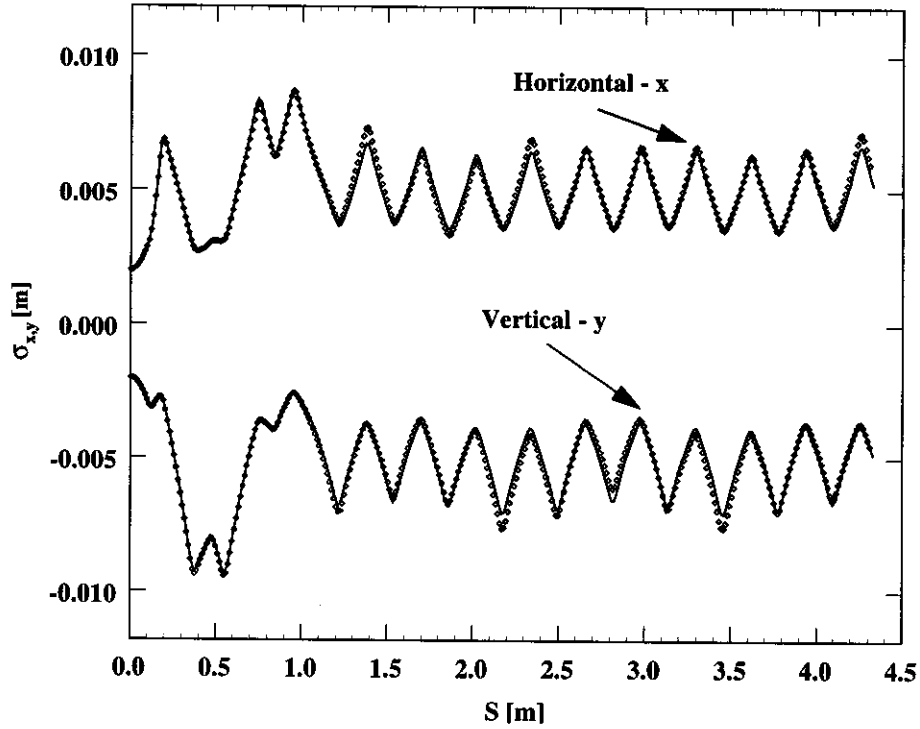


**Figure 4.** Results of PIC-simulation in free space for  $Q=1.5 \times 10^{-3}$  and  $\sigma_8 = 1.5 \times 10^{-2}$ . Shown are rms envelopes  $\sigma_{x,y}$  from the envelope-based code and rms values derived from particle tracking with the PIC code with dimensions in meters.

The standard rms emittance  $\epsilon_x(s) = \sqrt{\langle x^2 \rangle \langle p_x^2 \rangle - \langle xp_x \rangle^2}$  is not generally conserved in a dispersive system. Plotted in Figure 5 are the effective emittances  $E_x$  and  $E_y$  from the envelope-based code and from the PIC code ( $E_{x,y} = 4\epsilon_{x,y}$ ).

A generalized emittance invariant in the context of the rms envelope model is<sup>3</sup>:

$$\epsilon_{dx}^2 = (\langle x^2 \rangle - D^2 \langle \delta^2 \rangle)(\langle p_x^2 \rangle - D'^2 \langle \delta^2 \rangle) - (\langle xp_x \rangle - DD' \langle \delta^2 \rangle)^2, \text{ or}$$

$$\epsilon_{dx}^2 = \epsilon_x^2 - \langle \delta^2 \rangle \langle p_x D(z) - x D'(z) \rangle$$

The quantity  $D$  is the dispersion function plotted (dotted) in Figure 2.

The behavior of the effective generalized emittance ( $E_{dx} = 4 \varepsilon_{dx}$ ) from the PIC simulation, a strict invariant for the rms envelope model, is also given in Figure 5 showing non-invariant behavior with a growth of about 50%. In the envelope-based model,  $\varepsilon_{dx}$  is coincident with  $\varepsilon_y$ -Envelope.

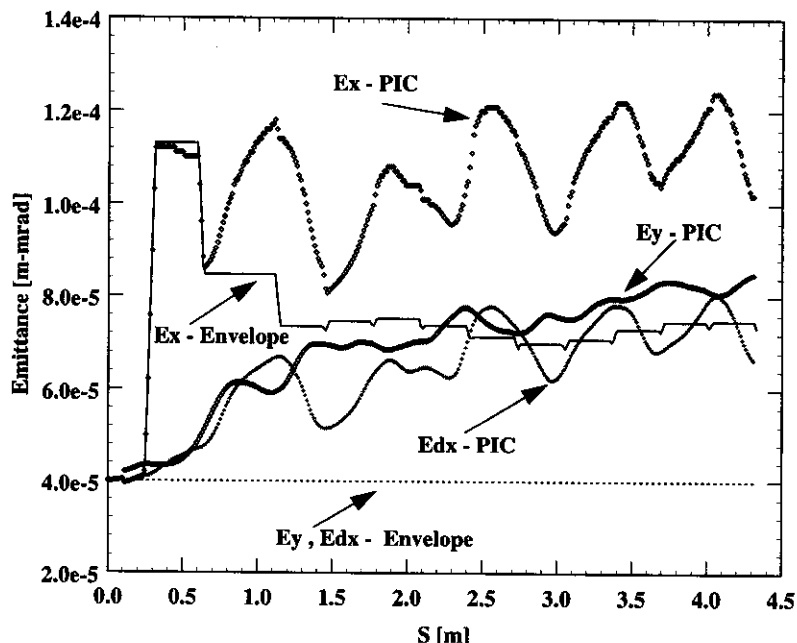


**Figure 5.** Effective emittances from PIC simulation in free space and from envelope model for the case:  $Q=1.5 \times 10^{-3}$ ,  $\sigma_\delta=1.5 \times 10^{-2}$ . The generalized emittance is also shown.

For a specific  $i$ -th particle with coordinate  $x_i$  and momentum  $p_i$ , the dispersion functions may be defined as:  $D_{i,x} = (x_i - x_0) / \delta_i$  and  $D'_{i,x} = (p_i - p_0) / \delta_i$ , where  $x_0$  and  $p_0$  denote the reference particle coordinate and its momentum. In the presence of space charge, each particle, strictly speaking, has it's own dispersion and a mean dispersion for the particle ensemble should be found. One approach is to perform the averaging for an ensemble of  $I$  test particles  $i = 1, 2, \dots, I$  using<sup>3</sup>:

$$\langle D_x \rangle = \langle (x - x_0) \delta \rangle / \langle \delta^2 \rangle \quad \text{and} \quad \langle D'_x \rangle = \langle (p_x - p_0) \delta \rangle / \langle \delta^2 \rangle$$

Three dispersion functions are given in Figure 6; one from the rms envelopes and two from the PIC simulation for a single particle ( $D_{i,x}$ ) and an ensemble average ( $\langle D_x \rangle$ ). The agreement between the dispersion derived from envelope-based model and the average dispersion  $\langle D_x \rangle$  obtained from analysis of the tracked particles is excellent. The number of the test particles ( $I$ ) was 10. The dispersion corresponding to an individual

particle  $D_{i,x}$  provides good initial agreement until the injection point ( $s = 1.15$  m), but after that differs significantly.

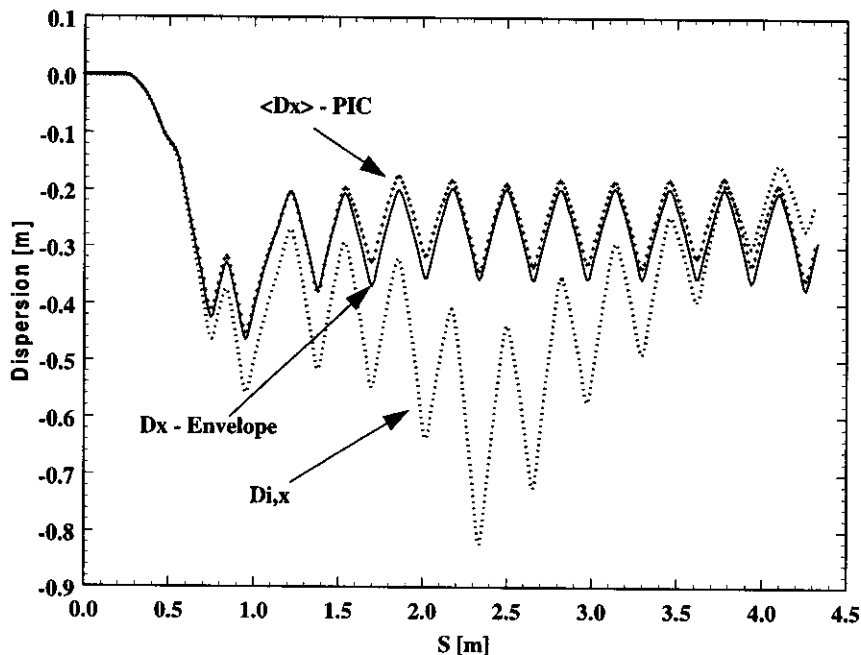


**Figure 6.** Dispersion function for the 3rd case from envelope equation model and dispersion functions  $\langle D_x \rangle$  and  $D_{i,x}$ , calculated by PIC simulation for a momentum spread of  $\Delta p_i / p = \pm \sigma_\delta = \pm 0.015$ .

Non-dispersive injection into the E-Ring was also considered with the layout envelope-based results shown in Figure 7. Since the dispersion can not be matched in a bend-free injection line, the beam experiences perturbations in the periodical E-Ring structure<sup>2</sup>.

The dynamics of the second moment ( $\sqrt{\langle x^2 \rangle}$  and  $\sqrt{\langle y^2 \rangle}$ ) again showed good agreement between the envelope-based analysis and the PIC particle tracking. The emittances for this case are given in Figure 8 where the generalized emittance again shows a non-invariant behavior with  $\approx 50\%$  increase. The emittances are significantly greater than those of Figure 5, possibly leading to difficulties in interpreting experimental results.

The dispersion functions are given in Figure 9 where the envelope-based and PIC simulation derived values show less agreement for this case as compared to that shown in Figure 6.

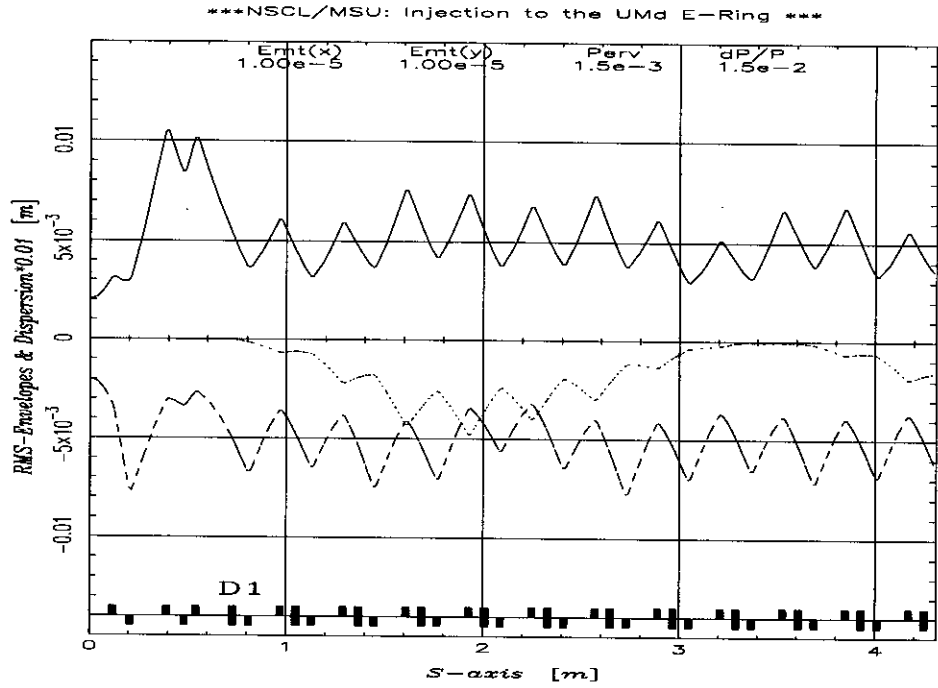


**Figure 7.** RMS beam envelopes  $\sigma_x$  (solid line - horizontal) and  $\sigma_y$  (dashed line -vertical) and dispersion function  $D_x$  (dotted line) for  $Q = 1.5 \times 10^{-3}$  and  $\sigma_\delta = 1.5 \times 10^{-2}$  for the case of a bend-free injection line.  $\sigma_{x,y}$  are perturbed due to absence of dispersion matching.

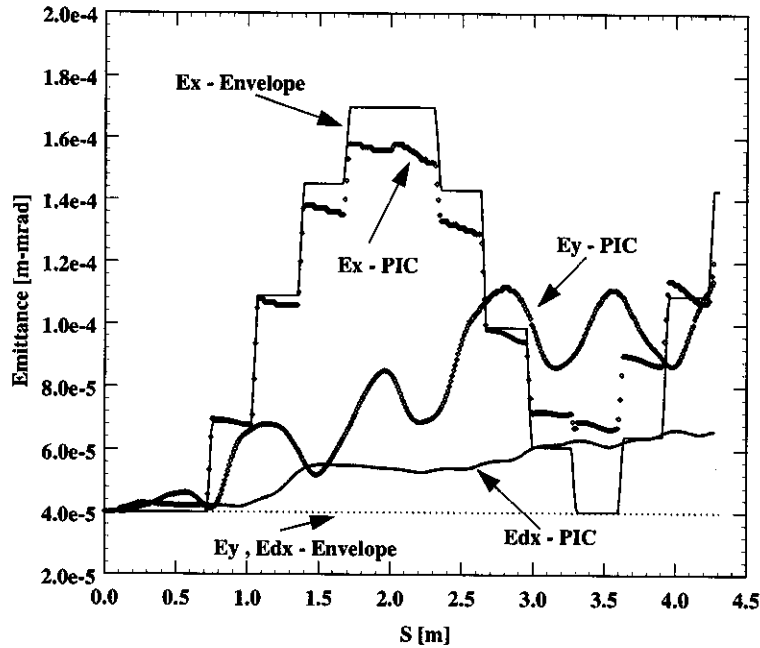


**Figure 8.** Effective emittances from PIC simulation and from envelope-based model for the case of  $Q = 1.5 \times 10^{-3}$ ,  $\sigma_\delta = 1.5 \times 10^{-2}$ , and a bend-free injection line.



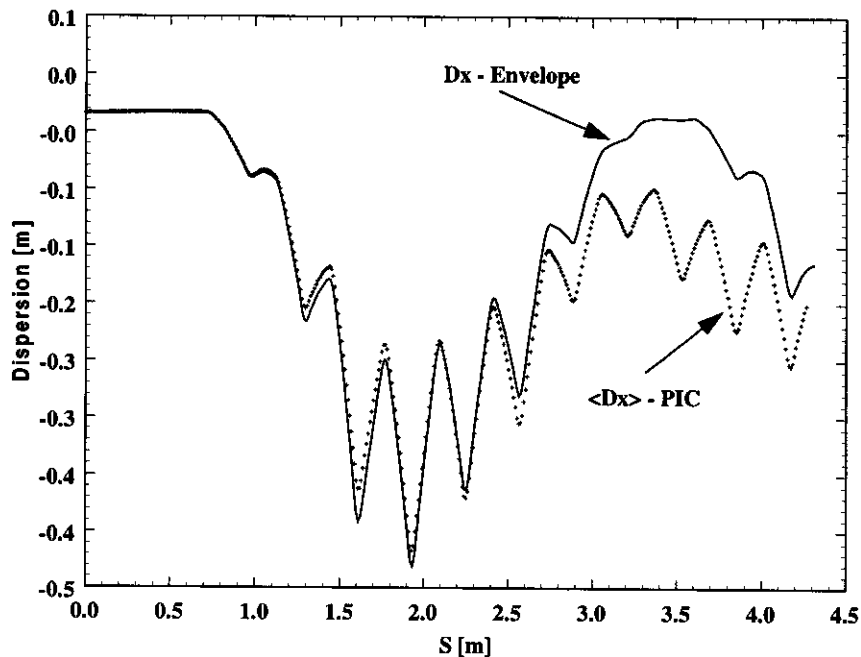


**Figure 9.** The dispersion functions: from rms envelope equations and  $\langle D_x \rangle$ , for the bend-free injection system of Figure 7.

## 5. Conclusion

A fitting algorithm based on rms-envelope equations was developed that has proved to be fast and flexible matching up to  $6 \times N$  fitting constraints simultaneously (where  $N$  is the number of locations; in practice  $1 \leq N \leq 4$ ). The PIC code was improved allowing the comparison between the envelope-based model and particle tracking. The rms envelopes from the envelope-based and the PIC code showed good agreement showing the success of the envelope-based model and coincidentally providing some verification of the PIC program. The evolution of  $E_{x,y}$  and  $E_{dx}$  from PIC simulation can be used to determine the limits of validity of the generalized rms envelope equations and possibly point to an improved model.

In the future, the 2D PIC code will be completed with the implementation of the following improvements.

- General rectangular magnets will be implemented.
- A fringe field model for the magnetic elements will be included.
- The speed of the Poisson solver will be improved.
- Numerical data filtering will be introduced.
- An acceleration element will be included.

Following these improvements to the 2D PIC code, implementation of the longitudinal dynamics will be done via the slice technique as described in reference 4.

## References

- 1 M.Reiser et al. "The Maryland Electron Ring for Investigating Space-Charge Dominated Beams in a Circular FODO System", PAC'99 Conference, New York (1999), p. 234. See also <http://www.ipr.umd.edu/ebte/ring/>
2. L.G.Vorobiev and R.C.York "Analysis of the Injection Line for the University of Maryland Electron Ring Including Dispersion and Space Charge", MSUCL-1122, (1999).
3. M.Venturini, R.A. Kishek and M.Reiser "Dispersion and Space Charge", Shelter Island Workshop on Space Charge, AIP Proc. 448 (1998) p. 278.
4. L.G.Vorobiev and R.C.York "Calculation of longitudinal fields of high-current beams within conducting chamber", PAC'99 Conference, New York (1999), p. 2781.